Supplementary Information: Phase behavior and design rules for plastic colloidal crystals of hard polyhedra via consideration of directional entropic forces†

A. S. Karas,[a] J. Dshemuchadse,[a] G. van Anders,[b] and S. C. Glotzer*[a,c,d]

1 Comparison of preferential orientations for RD and RC

Figs. S1 and S2 display the probability of finding particles in systems of rhombic dodecahedra (RD) or rhombicuboctahedra (RC) in specific orientations as a function of density. The effect of RD having only the 12 FCC-relevant bonding facets *vs.* RC having an additional 14 non-bonding facets can be seen in these plots. For RC, the non-bonding facets lead to the existence of additional orientations (the '63° defect' orientations in Fig. S2) that are incommensurate with the oFCC arrangement, but that occur more often in the pFCC than would be expected from a random set of orientations. For RD, we are unable to find such an orientation that preferentially exists in the pFCC but not in the oFCC crystal through simple geometric reasoning.

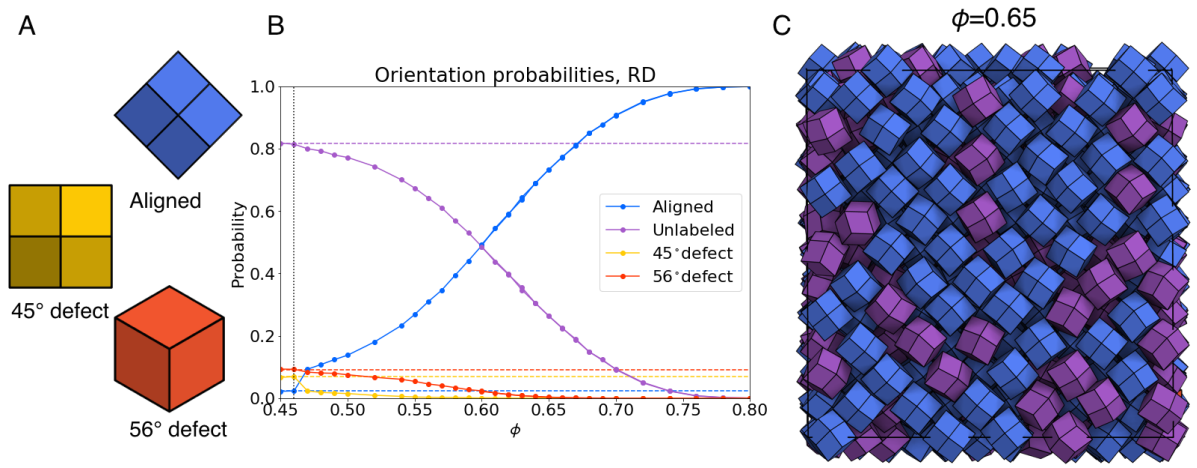

Fig. S1: *A* Examples of the three types of orientations that we distinguish for RD. We classify whether a particle fits into one of these categories if its orientation is within a 15° cutoff. 'Aligned' refers to particles with the orientation that occurs in the densest packing. '45° defect' refers to particles rotated by 45° about one of the three principal (4-fold) axes of the particle relative to the 'aligned' orientation. '56° defect' refers to orientations in which a 3-fold vertex has replaced a 4-fold vertex relative to the 'aligned' orientation. *(B)* The probability of finding these different orientations as a function of density. 'Unlabeled' refers to all particles whose orientations do not fit within the 15° cutoff of these specific orientations. The dotted horizontal lines signify the probability of finding the different orientations in a random distribution. For RD, only the 'aligned' orientations appear more frequently than would be expected in a random distribution. At $\phi = 0.47$, the increase in probability for 'aligned' particle orientations corresponds to the transition from a fluid to the pFCC crystal. *(C)* An example snapshot of a system at $\phi = 0.65$ with the particles colored by orientation.

[a] *Department of Chemical Engineering, University of Michigan, Ann Arbor, Michigan 48109, USA.*
[b] *Department of Physics, University of Michigan, Ann Arbor, Michigan 48109, USA.*
[c] *Department of Materials Science and Engineering, University of Michigan, Ann Arbor, Michigan 48109, USA.*
[d] *Biointerfaces Institute, University of Michigan, Ann Arbor, Michigan 48109, USA. E-mail: sglotzer@umich.edu*
† Article available at DOI: XXXXXXXXXX

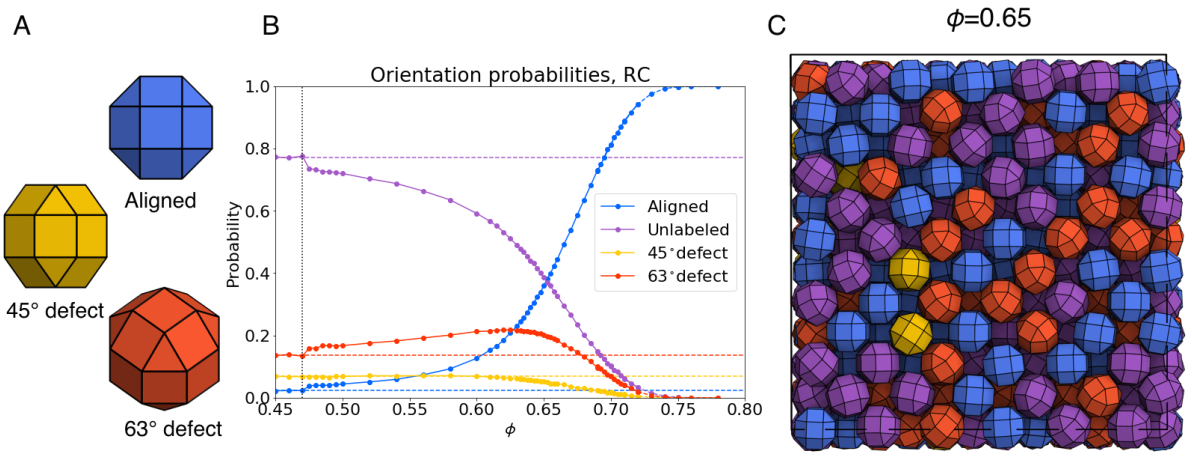

Fig. S2: *(A)* Examples of the three types of orientations that we distinguish for RC. We classify whether a particle fits into one of these categories if its orientation is within a 15° cutoff. 'Aligned' refers to particles with the orientation that occurs in the densest packing. '45° defect' refers to particles rotated by 45° about one of the three principal (4-fold) axes of the particle relative to the 'aligned' orientation. '63° defect' orientations can be attained *via* two separate 45° rotations about separate axes. *(B)* The probability of finding these different orientations as a function of density. 'Unlabeled' refers to all particles whose orientations do not fit within the 15° cutoff of these specific orientations. The dotted horizontal lines signify the probability of finding the different orientations in a random distribution. At $\phi = 0.475$, there is an increase in probability for 'aligned' and '63° defect' corresponding to the transition from a fluid to the pFCC crystal. Below a density $\phi = 0.67$, '63° defect' orientations occur more frequently in a system of RC than would be the case in a random distribution of orientations. *(C)* An example snapshot of a system at $\phi = 0.65$ with the particles colored by orientation.

2 Coexistence of pFCC and BCT phases

We compute the equation of state in the vicinity of the pFCC-to-BCT transition for systems sizes $N = 256$, 2048, & 16384 to confirm that the height of the Mayer-Wood loop decreases with system size. These results are shown in Fig. S3(*A*). A Mayer-Wood loop appears as a result of coexistence between the two phases[1]. Figs. S3(*B & C*)) show coexistence behavior based on local density for two different system sizes of TC. Coexistence of the pFCC and BCT crystals is identified when there are two distinct peaks in the local density of a system. These results help confirm that the transition in Fig. 3 is of first order.

3 No continuous phase transition in RC systems

The equation of state for RC shows a distinctive near-flattening in the density range $0.68 < \phi < 0.73$ (see main text). We have performed simulations at various system sizes to show that this feature does not correspond with a higher order phase transition. In a second-order phase transition, we expect to see discontinuities in a derivative of F, the free energy[2]. In an *NVT* ensemble, wherein $P = -(\frac{\partial F}{\partial V})$, the bulk modulus K is a second-order derivative:

$$K = -V\frac{\partial P}{\partial V} = V\frac{\partial^2 F}{\partial V^2}. \tag{1}$$

Fig. S4 shows the bulk modulus plotted against density for $N = 256$, 864, & 16384. We do not find any change in the bulk modulus as a function of system size. If there were a critical phenomenon associated with a higher order phase transition, we would expect to see divergence as the system approached the thermodynamic limit.

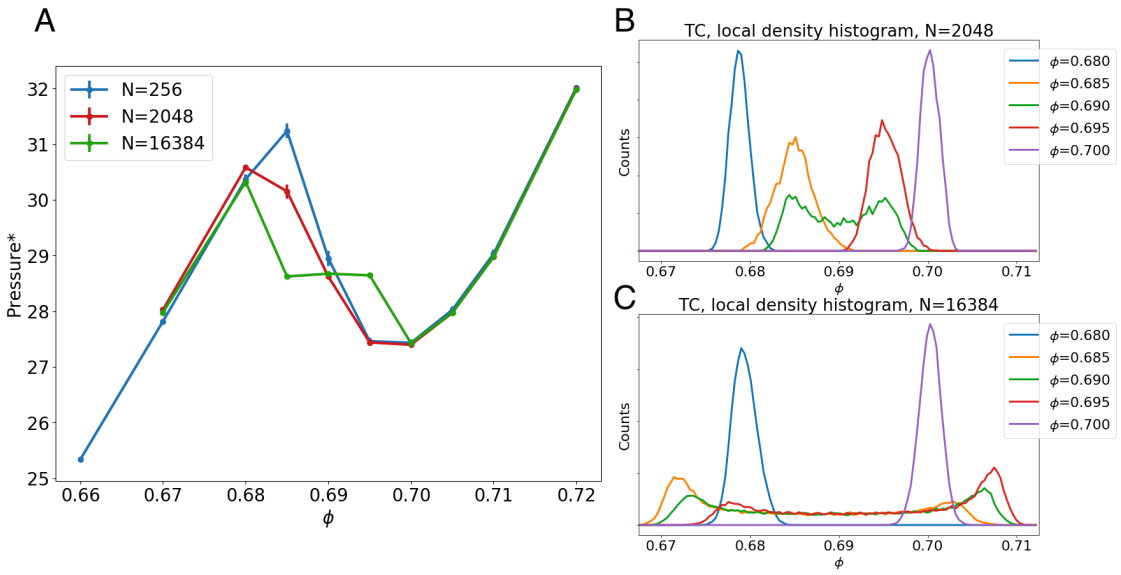

Fig. S3: Evidence of a first-order phase transition for TC. *(A)* Equation of state from *NVT* simulations as a function of system size. The decrease in the size of the Mayer-Wood loop with system size is the result of two-phase coexistence and comparatively fewer particles being located at the interface. *(B)* For system sizes $N = 2048$, coexistence is only observed at a density of $\phi = 0.69$. *(C)* For system sizes $N = 16384$, the system will separate into the pFCC and BCT phases when the total density is $0.685 \leq \phi \leq 0.695$.

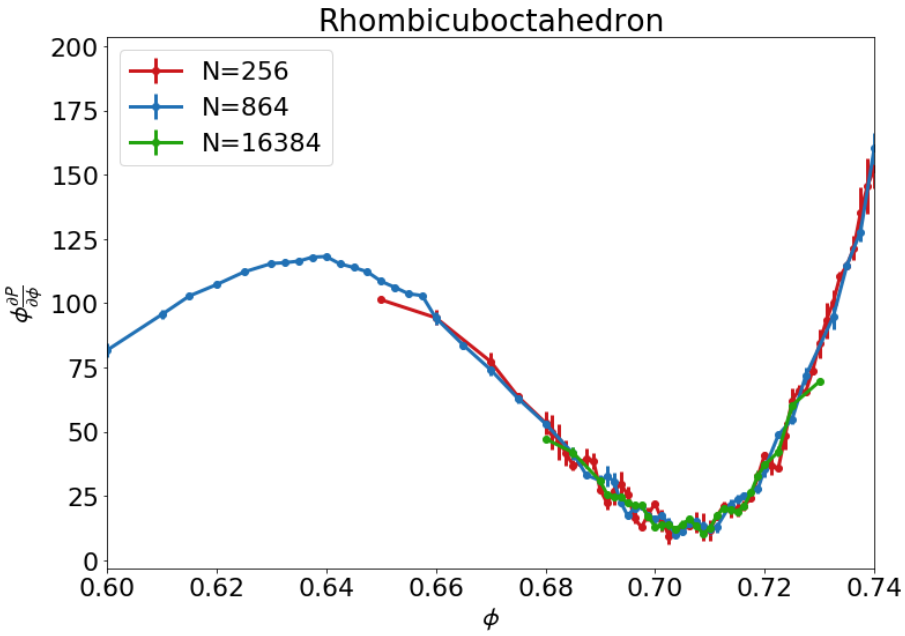

Fig. S4: Bulk modulus of RC for system sizes $N = 256$, 864, & 16384. The value of the bulk modulus does not depend on system size, which indicates that there is no continuous phase transition.

4 Rotational Autocorrelation Function

The dynamics of particle translations is frequently characterized through the self-part of the intermediate scattering function, which is the Fourier transform of the van Hove function. To characterize rotational dynamics, we seek a similar description. However, whereas the space of possible translations is described by $\mathbb{R}$, the space of possible rotations is described by the manifold of the rotation group, SO(3), requiring a different form of Fourier transform. For convenience, we note that SU(2) is the double cover of SO(3), and that SU(2) has the group manifold S^3, so we can study rotational

dynamics by doing a Fourier transform in terms of spherical harmonics on S^3. In particular we define

$$F_l(t) = \frac{1}{N} \sum_i \sum_{m_1 m_2} Y^*_{l m_1 m_2}(0) Y_{l m_1 m_2}(q_i(0)^\dagger q_i(t)) \,, \tag{2}$$

where $Y_{l m_1 m_2}$ are spherical harmonics, q_i is the orientation of particle i, and the summation extends over all particles and the magnetic quantum numbers m_1, and m_2. In our calculations, we set $l = 6$.

To compute $F_l(t)$ we used conventions for $Y_{l m_1 m_2}$ similar to those given in Ref.[3]. In particular, we embed S^3 in $\mathbb{R}^4$ using the complex coordinates ξ and ζ. For a unit quaternion defined by $q = w + xi + yj + zk$, we follow Ref.[3] and use this parameterization:

$$\begin{aligned} \xi &= x + iy, \\ \zeta &= z + iw. \end{aligned} \tag{3}$$

If we sum over all possible quantum numbers and use $a = -(m_1 - \frac{l}{2})$ and $b = -(m_2 - \frac{l}{2})$, we represent the spherical harmonics by summing over all non-negative exponents for the following expression[3]:

$$Y_{l, \frac{l}{2}-a, \frac{l}{2}-b} = \sqrt{\frac{a!(l-a)!b!(l-b)!}{l+1}} \sum_k \frac{(\xi^*)^k \zeta^{b-k} (\zeta^*)^{a-k} (-\xi)^{l+k-a-b}}{k!(l+k-a-b)!(a-k)!(b-k)!} \,. \tag{4}$$

The results of computing the rotational autocorrelation function across a wide density range with constant rotational move size are included in Fig. S5. As would be expected, the number of sweeps required for a particle to forget a past orientation monotonically increases with density. With all shapes, two-step behavior in the rotational autocorrelation function develops at high densities. This two-step behavior is indicative of cage-like rotational motion: at high densities, particles can not readily make large rotations. Instead, they mostly make small rotations about an averaged orientation. A set of rotational moves that takes particles outside of this cage can occur, but it happens infrequently at high densities.

For all shapes in this study, change in behavior of the rotational autocorrelation function shows connections with the development of orientational order. For the TC (Fig. S5(*A*)), the development of two-step behavior coincides with the pFCC-to-BCT phase transition. With the gradual order development displayed by the RD and RC (Fig. S5(*B* & *C*)), the rotational autocorrelation function helps to confirm the development of strong orientational order and the loss of plastic crystal behavior shown at lower densities. At low densities, the rotational autocorrelation function shows exponential decay, and at higher densities with greater order the two-step behavior develops. The dynamic behavior of the PRC suggests the orientational glass transition upon compression. For the highest density statepoint initialized with FCC order in Fig. S5(*D*) (the dark green curve for $\phi = 0.725$), there is clear two-step behavior in the rotational autocorrelation function suggesting caged motion and the beginnings of dynamical arrest in rotational motion.

We find that the behavior of the rotational autocorrelation function matches with results from the orientation-orientation coupling across all shapes studied here. Specifically, the density at which two-step behavior develops corresponds with the vanishing probability of misorientation angles corresponding to intermediate configurations. This connection makes intuitive sense: if particles are experiencing caged rotational motion, then the intermediate configurations which lead to changes in orientation will be rare events as measured by the orientation-orientation coupling.

References

1 J. E. Mayer and W. W. Wood, *The Journal of Chemical Physics*, 1965, **42**, 4268–4274.

2 N. Goldenfeld, *Lectures On Phase Transitions And The Renormalization Group (Frontiers in Physics)*, Addison-Wesley, 1992.

3 R. E. Cutkosky, *Journal of Mathematical Physics*, 1984, **25**, 939–942.

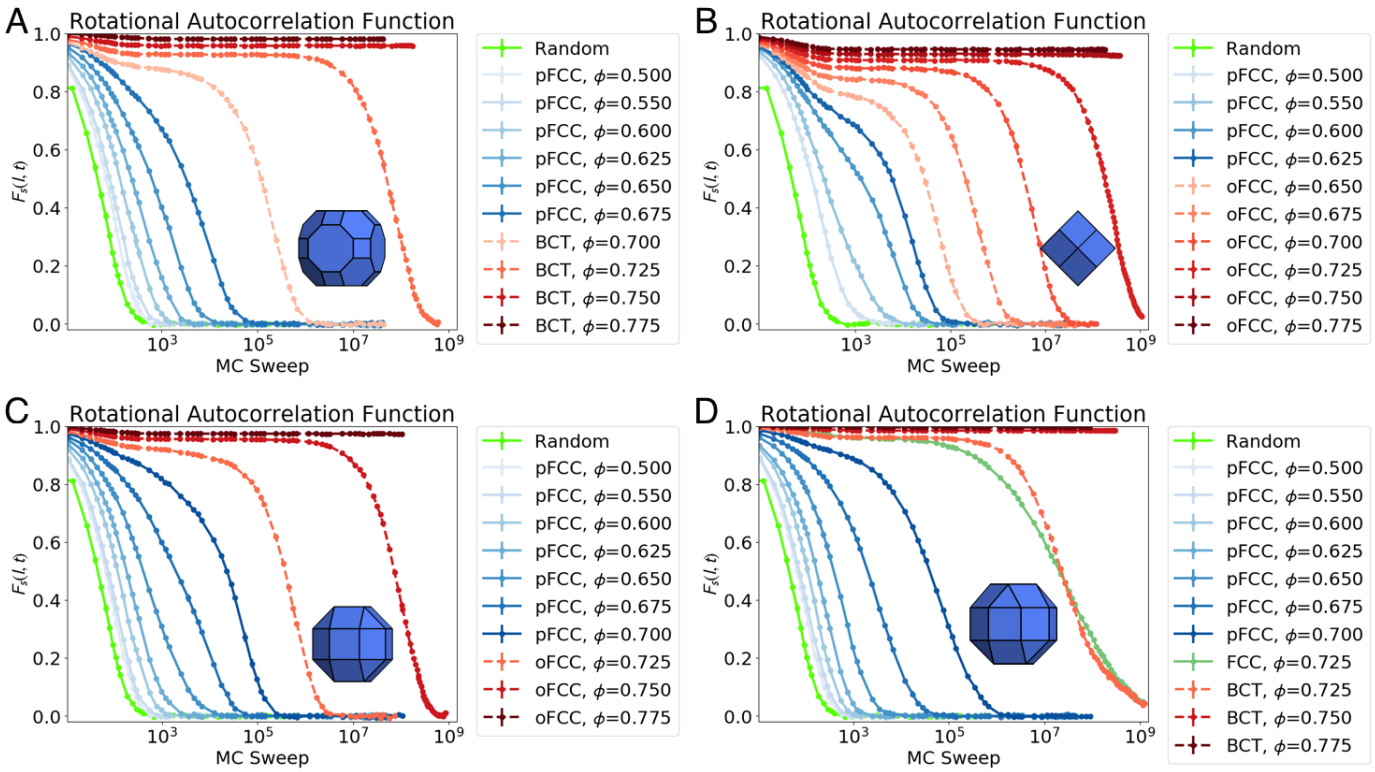

Fig. S5: The rotational autocorrelation function calculated with $l = 6$ (right) for all shapes. The light green curve labeled 'Random' corresponds to free, unhindered rotations. *(A)* For the TC, two-step behavior develops at the transition to a BCT crystal. For the gradual order development in shown by RD *(B)* and RC *(C)*, the development two-step behavior helps to define the loss of plastic crystal behavior. *(D)* For the PRC, neither the FCC or BCT-initialized states show plastic crystal behavior and instead have two-step behavior and long time scales for the decay in the rotational autocorrelation function.